Highly Oriented Mesoporous Silica Channels Synthesized in Microgrooves and Visualized with Single-Molecule Diffusion

Bastian Rühle,[†] Melari Davies,[†] Timo Lebold, Christoph Bräuchle,[*] and Thomas Bein[*]

Department of Chemistry and Center for NanoScience (CeNS), University of Munich (LMU), Butenandtstrasse 5-13 (E), D-81377 Munich, Germany.
[†]These authors contributed equally to this work

ABSTRACT A novel synthesis method for large-pore, well-aligned 2D hexagonal mesoporous silica thin films is reported. The alignment was achieved by confinement in poly (dimethylsiloxane) (PDMS) microgrooves without the necessity of additional forces (such as electric fields). We describe the influence of various experimental conditions including the way the grooves are filled, surface modification at the solid/liquid interfaces, and the height-to-width ratio of the microgrooves on mesopore alignment. With this technique, highly oriented mesoporous silica channels can be obtained at a length scale of several millimeters. For a nondestructive, detailed, and wide-ranging structural and dynamic characterization of the as-synthesized mesochannel silica network, dye molecules were incorporated into the channels at concentrations suitable for single-molecule microscopy. A "maximum projection" of individual frames recorded with a fluorescence microscope immediately gives a global overview ("map") of the pore structure, thus providing direct feedback for tuning synthesis conditions. In addition, deeper insights into the real nanoscale structure of the mesoporous silica framework were obtained through high-accuracy single-molecule tracking experiments. The high spatial accuracy of the experiments allowed for the direct observation of jumps of single dye molecules between individual channels in the mesoporous silica host. Nevertheless, due to the low concentration of defects, the diffusion could be described as a 1D random walk where the molecules diffuse along the highly oriented, parallel channels and sometimes switch from channel to channel through small defects in the pore walls. Furthermore, it could be shown with single-molecule microscopy that template removal and calcination of the aligned films results in an increased defect concentration; however, the overall order of the structures remained intact.

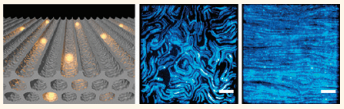

KEYWORDS: mesoporous silica · thin films · pore alignment · single-molecule studies · fluorescence microscopy

Two-dimensional hexagonal (*p6mm*) mesoporous silica materials have attracted much attention as a host for versatile applications including nanofluidics and nanoreactors,[1] oriented growth of nanowires,[2] and optoelectronic devices.[3] For these applications, control over pore alignment can be crucial. However, the evaporation-induced self-assembly (EISA) approach,[4] which is one of the most common ways to prepare these structures, usually results in small domains with randomly oriented mesoporous channels. This can be attributed to the lack of a preferential direction on the substrate, and a variety of ways have been reported aimed at introducing a preferential direction of the mesopores on a macroscopic scale, including microtrenches,[5] external electric[6,7] and magnetic fields,[8] substrate surface modification,[9] and shear flow control.[10] However, these approaches often require specialized equipment or impose constraints on the applicable substrates or surfactants. In the case of employing microtrenches, a clean room and a photolithography or even an electron-beam lithography setup is needed, rendering these approaches costly and time-consuming. The use of external fields requires charged templates such as CTAB, hence limiting this approach to mesoporous silica with small pores. The other approaches require crystalline substrates with a certain crystallographic orientation or result in channel lengths typically <1 μm. In this contribution, we describe a general approach for the design of oriented mesoporous silica films with large pores and large channel length (typically around 10 μm) that serve as model systems for the investigation of single-molecule diffusion. This approach is not limited by the need for specific substrates (*e.g.*, nonconductive substrates or substrates with crystalline order), specific templates (*e.g.*, ionic surfactants), or the application of strong electric or magnetic fields that may be difficult to implement. Moreover, to the best of our knowledge, this is the first report of an in-depth investigation of the structural features (such as correlation length and domain sizes) and

* Address correspondence to Christoph.Braeuchle@cup.uni-muenchen.de, tbein@cup.uni-muenchen.de.

Received for review July 10, 2011 and accepted January 23, 2012.

Published online January 23, 2012
10.1021/nn2042835

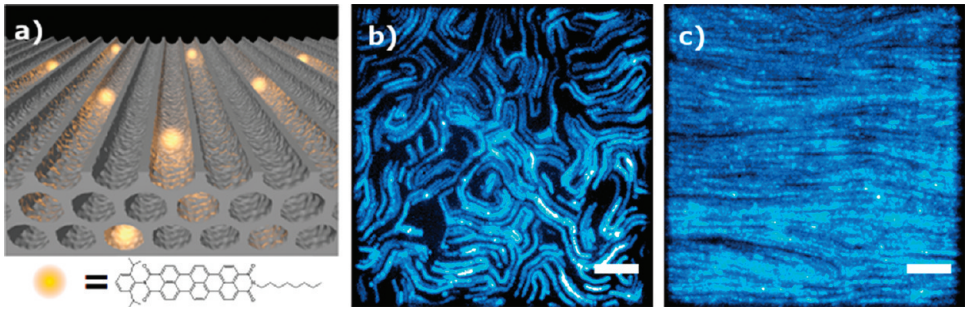

Figure 1. Representation of schematic structure and different domain patterns in the mesoporous thin films. Schematic representation of fluorescent dye molecules diffusing inside 2D hexagonally arranged mesopores of a porous silica host (the template is omitted for clarity) (a, top) and the chemical structure of *N*-(2,6-diisopropylphenyl)-*N*′-octylterrylene-3,4,11,12-tetracarboxdiimide (As-TDI) (a, bottom). Maximum projection of the individual frames of a movie recorded with a fluorescence microscope at a frame rate of 2.5 fps taken from sample 1, revealing the ordering of the mesoporous structure (false-colored in blue; scale bars are 5 μm; see also movies M1 and M2 in the Supporting Information) (b,c). The cylindrical mesopores lie in a plane parallel to the substrate, but they do not show macroscopic in-plane alignment (b). The mesopores lie in a plane parallel to the substrate and show a preferential alignment (left-right) on a macroscopic length scale (c).

dynamical properties (such as guest diffusion) of large-pore silica materials with macroscopically aligned mesochannels.

Our approach was inspired by a technique initially introduced by Whitesides *et al.* as *micromolding in capillaries* (MIMIC),[6,7] where an EISA precursor solution is filled into microgrooves defined by a poly(dimethylsiloxane) (PDMS) stamp. This technique is, in principle, compatible with any flat substrate and any surfactant, and no specialized equipment is needed once the masters for the PDMS stamps are obtained. Moreover, the PDMS stamps can be reused, rendering this approach very simple, fast, and cost-effective. We extended the MIMIC approach and investigated mesopore alignment inside PDMS microgrooves using the well-known, uncharged Pluronic F127 triblock copolymer as a template. We found that the reaction conditions and the surface modification at the solid−liquid interfaces inside the microgrooves can drastically influence the direction of the mesopore alignment. We also introduce single-molecule fluorescence microscopy as a very efficient and powerful tool to gain direct insights into the mesochannel structure, correlation length, and pore directionality in the mesoporous silica films. This method provides unique nanoscale structural information about the pore system and about the interactions of guest molecules with the porous host that cannot be obtained with any other analytical technique (see also Results and Discussion section for a more detailed description of this concept).[11−14]

RESULTS AND DISCUSSION

Before the detailed description of the synthetic strategies and how different parameters can affect mesopore alignment, we present some general remarks about the 2D hexagonal (*p6mm*) silica structure itself and the way single-molecule fluorescence microscopy is used as a fast and efficient tool to investigate mesopore alignment and correlation length. It is known from the literature that an EISA precursor solution of the composition described below (see Experimental section) can give a 2D hexagonal phase of mesoporous silica with cylindrical (or elliptical) mesopores lying preferentially in a plane parallel to the substrate.[15] These structures are commonly characterized using X-ray diffraction (XRD) or (cross-sectional) electron microscopy techniques. However, a simple 1D XRD pattern can only give information about the phase (hexagonal or cubic) of a mesoporous silica thin film but says little about its in-plane ordering or the domain sizes. More elaborate X-ray diffraction techniques can also give information about the pore directionality of the mesopores, but these techniques also do not provide much information about the domain size and correlation length of the cylindrical mesopores, and they give only averaged data for a certain area without spatial resolution. On the other hand, electron microscopy top view images of the structure can give information about the phase, the alignment and—to some extent—the correlation lengths of the individual mesopores. However, this only works for the topmost layer in scanning electron microscopy (SEM) (or thin layers in transmission electron microscopy (TEM)), but as will be shown in this work, the alignment of the mesopores can differ drastically between top and bottom layers. In contrast, cross sections can provide information about the orientation at different heights, but they do not directly provide information about domain sizes of the mesopore channels and they usually require destruction of the sample.

Single-molecule fluorescence microscopy can complement XRD and electron microscopy data[12] and directly provide spatially resolved information about alignment and correlation lengths of mesoporous channels in a fast, direct, and nondestructive way. Moreover, several additional parameters such as the diffusion coefficient of the fluorescent dyes inside the

mesopores or even information about defects in the mesoporous structure can be obtained, as will be shown later. In order to gain information about pore directionality and correlation length, we mixed a fluorescent dye (*N*-(2,6-diisopropylphenyl)-*N*′-octylterrylene-3,4,11,12-tetracarboxdiimide (As-TDI)) at a very low concentration (typically 10^{-10} to 10^{-11} M) into the EISA precursor solution. During self-assembly of the mesoporous silica structure, the hydrophobic dye is incorporated into the hydrophobic core of the micelles inside the cylindrical mesopores. After solidification of the silica network, the dye remains mobile inside the mesopores, presumably due to the presence of the template acting as a lubricant phase. However, the diffusional movement of the dye molecules is now confined by the silica side walls, so each of the "trapped" dye molecules moves inside a mesoporous channel network, exploring and mapping out the possible pathways. The positions of the dye molecules at different points in time hence create a "map" of the mesoporous structure inside the silica host (Figure 1).

This map can be obtained by recording a movie at the desired position of the sample with a fluorescence microscope (in this work, typically 200−1000 images at a frame rate of 2.5 frames per second (fps) were used) and subsequently overlaying the individual frames of the movie in an appropriate way (see next paragraph). This overlay shows directly that the dye molecules do not perform a random walk movement as it would be expected for dye molecules that are merely adsorbed on a surface or, to some extent, dye molecules inside a cubic (*Im*3*m*) structure, but they rather show a confined movement along certain pathways. Moreover, pore directionality and correlation length can also be directly obtained by analyzing the overlays. The fact that the dye molecules do not diffuse in and out of focus during the recording period of the movies shows that they are inside the 2D hexagonal mesoporous network with the pores aligned preferentially in a plane parallel to the substrate.

The most direct way of creating these overlays would be a summation of (or averaging over) the individual frames of the movie. While this technique works in principle, it has some drawbacks. Most importantly, it overemphasizes stationary fluorescent objects (*e.g.*, constant background, contaminations, immobile dye molecules, defects, *etc.*) compared to (fast) moving objects because a moving object only contributes intensity to a certain pixel of the overlay when it passes exactly this point in one of the frames of the movie (which might only be the case for a small fraction of the total frames), while a stationary object contributes the same intensity in each frame. For this reason, we used a "maximum projection" in this work, where each pixel in the overlay assumes the maximum value of the corresponding pixels in the individual frames that was reached during the recording time.

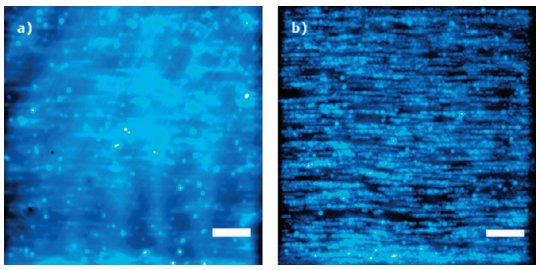

Figure 2. Two different ways of obtaining the overlay: by averaging over the individual frames (a) and by using a maximum projection (b). Both images are reconstructed from the same movie taken from sample 2, false-colored in blue, and contrast and brightness were optimized. Both scale bars are 5 μm. The corresponding movie M3 can be found in the Supporting Information.

Hence, the final overlay consists only of the brightest pixels of the movie. This technique treats moving and stationary fluorescent objects more equal and usually provides information-rich images. It is, however, more prone to overemphasizing noise than the averaging method described above since a bright spot in the background that occurs in only one of the frames of the movie is likely to end up in the final overlay. However, with bright fluorophores and a high signal-to-noise ratio, this is usually not a problem (Figure 2).

In order to trigger mesopore alignment during the EISA process, the condensation of the precursor solution was performed in confined spaces defined by a PDMS stamp with a stripe pattern. Two different approaches were pursued that are depicted schematically in Figure 3. In the first approach ("stamping approach"), a droplet of the precursor solution was deposited on the substrate, the stamp was placed on the latter, and pressure was applied on the stamp in order to achieve dewetting of the surface and to transfer the pattern of the stamp. In the other case ("capillary flow approach"), the stamp was placed on the substrate first, and then a droplet of the precursor solution was applied to both ends of the stamp. The solution gets sucked into the microgrooves defined by the stamp and the substrate by capillary flow. After solidification of the solution, the stamps can be carefully peeled off to obtain the final structure.

In the course of this work, we varied different parameters to investigate their influence on mesopore alignment. In addition to the two approaches described above, we also varied the height-to-width ratio of the microgrooves, the surface modification of the stamp and the substrate, and the synthetic conditions during solidification of the silica framework.

When stamps with microgrooves of a height-to-width ratio of approximately 1:2 (*ca.* 1.5 μm high and 3.0 μm wide) were used in the stamping approach without further modification of the stamp or the substrate, we found that the mesopores inside the structure tend to align perpendicular to the long axis of the channel (Figure 4). This finding is somewhat surprising

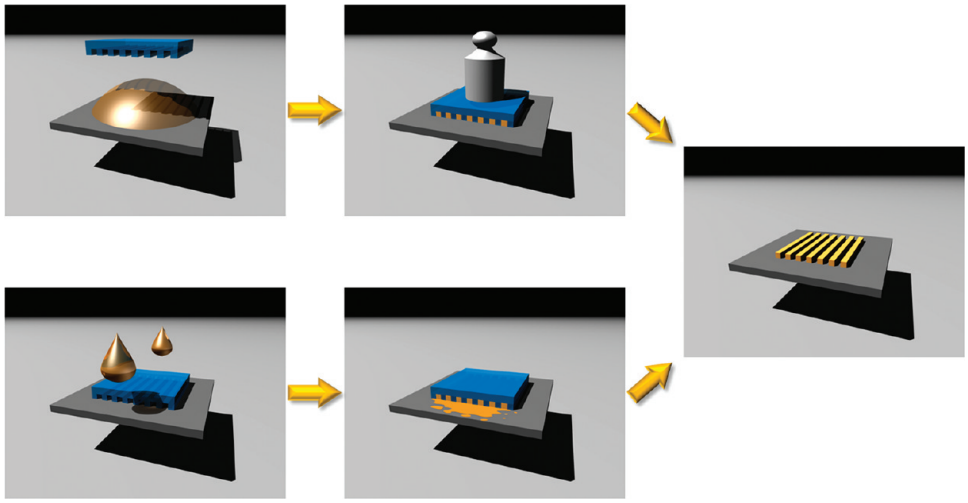

Figure 3. Schematic representation of the two approaches used to trigger mesopore alignment by confinement in PDMS microgrooves.

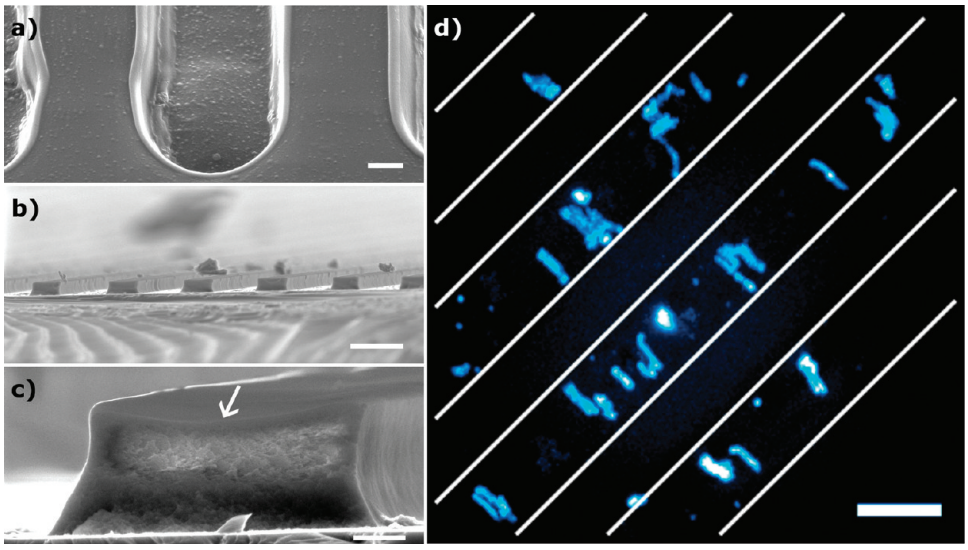

Figure 4. Microgrooves and silica mesopore patterns. Microgrooves in the PDMS stamp (scale bar is 1 μm) (a). Mesoporous silica pattern, produced by the "stamping approach" (scale bars are 5 μm and 500 nm, respectively) (b,c). In (c), the top surface of the silica bar is indicated by the arrow. Maximum projection through 500 individual frames of a movie recorded with a single-molecule fluorescence microscopy setup at 2.5 fps taken from sample 3, indicating the orientation of the mesochannels (false-colored in blue; white lines indicate the direction of the microgrooves; scale bar is 5 μm; see also movie M4 in the Supporting Information) (d).

since according to Aksay *et al.* the formation of end-caps in self-assembled micelle cylinders is unfavored due to their high free energy of formation.[7]

As the original goal was to obtain long, well-aligned mesochannels (preferably longer than the microgroove width), we investigated the influence of different synthesis parameters in order to favor mesopore alignment along the long axis of the microgrooves. Endo *et al.* showed that in silicon trenches with hydrophobic side walls the mesochannels of SBA-15 films tend to align perpendicular to the long axis of the trenches,[21] while in trenches with hydrophilic side walls a parallel alignment was favored. Additionally, it was known from dip-coating experiments conducted by Okubo *et al.*[15] that shear forces can also influence the alignment of the mesochannels favoring pore directionality parallel to the direction of flow (*i.e.*, the dipping direction in their experiments).

With this in mind, we investigated the capillary flow approach, which can provide shear forces during filling of the microgrooves in the stamp, in combination with different modifications of the surface properties of stamp and substrate regarding their hydrophilicity and hydrophobicity. The surface properties of the stamp and the substrate can be varied independently. Modification of the stamp influences the solid/liquid interface at three side walls of the resulting microgrooves, while modification of the substrate influences one solid/liquid interface. Modification of the interfacial properties can indeed strongly influence the

alignment of the mesoporous channels. Of the four possible combinations for surface functionalization of the stamp/substrate pair (*i.e.*, hydrophilic/hydrophilic, hydrophilic/hydrophobic, hydrophobic/hydrophilic, and hydrophobic/hydrophobic), best results (meaning preferential alignment of mesochannels parallel to the microgrooves) were achieved by using substrates rendered hydrophobic with PFOTS and stamps rendered hydrophilic by exposure to oxygen plasma and subsequent incubation in an acidic aqueous solution of TEOS. Using this combination, very well aligned mesopores could be obtained in narrow microgrooves (typically with a height of 1.5 μm and a width of 10−15 μm, *i.e.*, a height-to-width ratio smaller than 1:7 to 1:10) in 60−80% of the cases. In some cases, parallel alignment could also be observed in extremely low height-to-width ratio grooves with a height of approximately 1.5 μm and a width of *ca.* 30 μm, that is, a ratio of 1:20 (Figure 5).

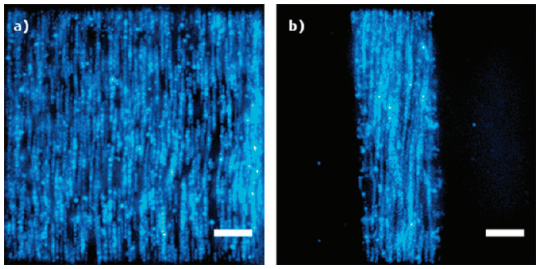

Figure 5. Maximum projection indicating the orientation of the mesochannels in a low height-to-width ratio channel (approximately 1:20; sample 2; rotated by 90° for clarity) (a) and a higher height-to-width ratio channel (approximately 1:6; sample 4) (b) (false-colored in blue; both scale bars are 5 μm; see also movies M3 and M5 in the Supporting Information).

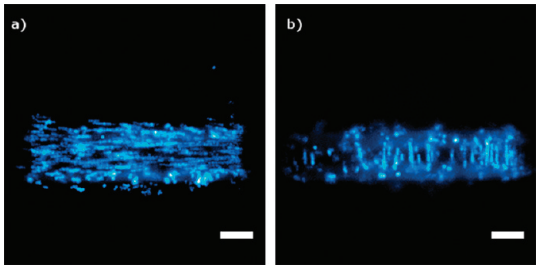

Figure 6. Maximum projection taken from sample 2, indicating the orientation of the mesochannels in a focal plane close to the substrate (a) and higher above the substrate (b) (false-colored in blue; both scale bars are 5 μm; see also movie M6 in the Supporting Information).

The parallel alignment usually extends over several millimeters from the ends into the interior of the microgroove, and under favorable circumstances, the entire resulting silica bar of 1−2 cm length showed alignment of the mesopores. The end regions differ from the middle region mainly in the following aspects. First, the capillary flow in these regions is stronger, indicated by the fact that the movement of the meniscus and hence the filling of the microgrooves occurs quite fast in the beginning (right after the droplet of the precursor solution was added to the open end of the stamp) but then rapidly slows down. Second, the supply with fresh reactants from excess solution that has not filled the microgrooves is better in these regions. Third, the evaporation rate of the solvent in these regions is different from the middle region since evaporation can occur easier through the open ends of the PDMS stamps.

Interestingly, in some cases, the pore directionality changed abruptly within one channel depending on the height above the substrate (*i.e.*, it changed within different focal planes of the microscope). While close to the substrate, an alignment parallel to the microgrooves could be observed, the orientation changed to a perpendicular alignment at higher positions (Figure 6).

We believe that this might be due to the fact that the silica patterns show a concave rather than a flat surface (see Figure 4c and Figure 7), and the alignment could follow this concave curvature. Similar observations were made by Endo *et al.* for dip-coated films in silicon microtrenches, and the authors attributed the effect to shear flow during solvent evaporation.[21]

We also observed that mesopore alignment parallel to the microgrooves can be achieved in higher microgrooves (4−8 μm height) by employing the "capillary flow approach" in combination with a hydrophobic

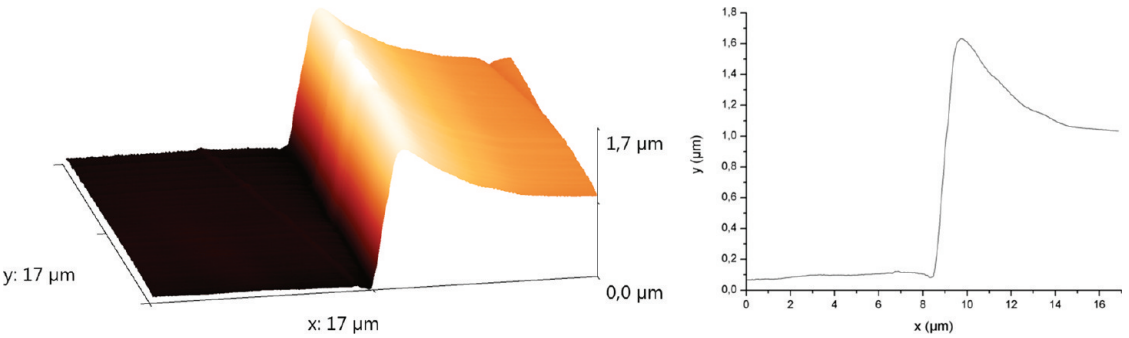

Figure 7. AFM Image and line profile from a silica bar showing its concave surface (sample 5); shown is one-half of the bar's cross section.

(*i.e.*, untreated) PDMS stamp and a hydrophilic substrate. This is interesting for the possible removal of the stamp by controlling the adhesion with the silica bar. In these experiments, we obtained results comparable to the ones shown above regarding mesopore orientation and correlation length when the samples are first incubated in a saturated atmosphere of ethanol at about 22 °C for 21 h and then additionally 24 h at ambient conditions (Figure 8). The saturated ethanol atmosphere slows down the evaporation rate of the solvent and hence the solidification of the silica matrix. However, after these aging times, the structures were found to be sufficiently stable to withstand mechanical stress (such as the stamp removal or SEM preparation) and further treatment such as extraction, and hence the solidification process, was considered to be complete after these times.

To determine the structure of the mesoporous silica in the microgrooves, small-angle X-ray scattering (SAXS) experiments and cross-sectional high-resolution scanning electron microscopy (HR-SEM) were performed (Figure 9). Both provide evidence for hexagonally arranged mesopores lying in a plane parallel to the substrate. The cross-sectional HR-SEM images (cleaved perpendicular to the microgroove direction) also indicate the well-ordered state of the mesopores along the long axis of a microgroove. The elliptical shape of the mesopores is typical because of the anisotropic shrinkage in mesoporous silica films during drying. Image analysis of the HR-SEM data gives a mean mesopore width of 6−8 nm and a height of 5−7 nm and a pore-to-pore distance of 12−16 nm horizontally and 9−13 nm diagonally, which is in line with the *d* spacing of the XRD (100) peak of *ca.* 7.5 nm.

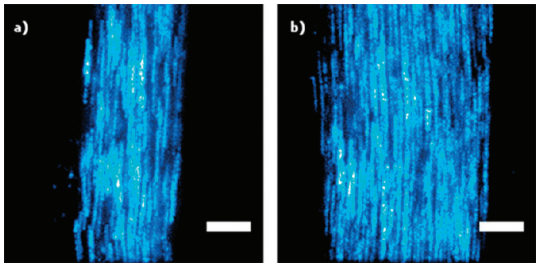

Figure 8. Maximum projection taken from sample 6, indicating the orientation of the mesochannels in silica bars of different widths prepared as described above (false-colored in blue; both scale bars are 5 μm; see also movies M7 and M8 in the Supporting Information).

Samples prepared in the way explained above (*i.e.*, samples 6−9) were also subjected to a more detailed analysis using single-molecule fluorescence microscopy. We obtained high spatial resolution for the pathways of single molecules inside the mesopores and thus could analyze the individual channel structures in much more detail. Furthermore, we could gain dynamic information about the diffusion of the molecules in such structures. The main driving force for molecular movement in these channel systems is Brownian motion, while biased motion due to concentration or structural gradients cannot be fully excluded.

In order to follow the pathway of single molecules with much higher accuracy, the dye concentrations were reduced even further than in the experiments performed before. A direct consequence of such low dye concentrations is the much better separation of the pathways of the single molecules from each other, as shown in Figure 10a.

Furthermore, such low concentrations increase the signal-to-noise ratio because of less background. Figure 10a shows the high contrast for the traces of 10 single molecules that can be obtained under such experimental conditions. The traces of 6 of these molecules were analyzed in greater detail and show a striking parallel alignment, thus indicating the high order of the silica channels at a large scale. Furthermore, the traces show different lengths whereby the trajectory of molecule no. 4 with 27 μm is one of the longest observed in our experiments. However, besides these well-ordered traces, some molecules diffuse in a random manner. These molecules are presumably at the surface of the sample where no guidance by the channel structure exists. Such behavior has been observed in previous studies[11] and is of no further interest here (movie M9 in the Supporting Information shows the movement of the molecules in Figure 10a in time lapse (10×)).

The pathway of a single molecule in Figure 10a was obtained by single-particle tracking, that is, the

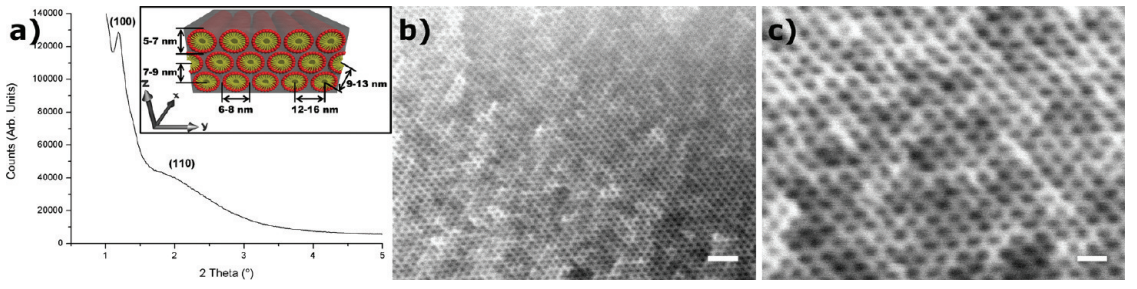

Figure 9. Structural analysis of the mesopore system of sample 7. XRD pattern (a) and cross-sectional HR-SEM images (cleaved perpendicular to the long axis of a silicon bar) of mesoporous silica produced as described above (b,c). Scale bars are (b) 50 nm and (c) 20 nm. The inset in (a) schematically illustrates the dimensions mentioned in the text.

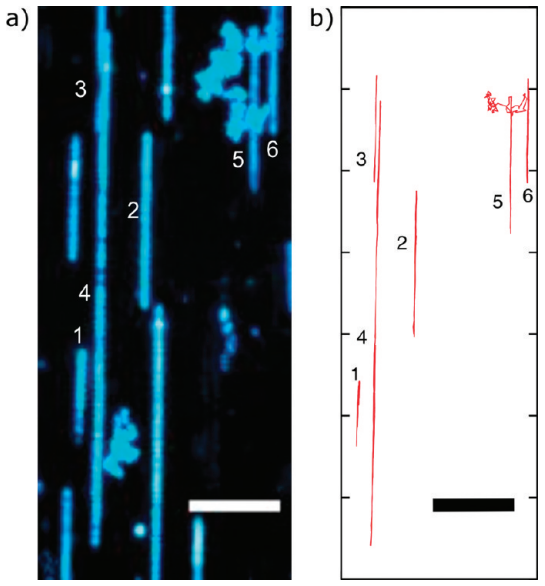

Figure 10. Maximum projection and trajectories of single molecules taken from sample 8. Maximum projection of the individual frames of a movie recorded with a fluorescence microscope at a frame rate of 2.5 fps, revealing the pathways of single molecules in the mesoporous structure (a). The mesopores lie in a plane parallel to the substrate and show a preferential alignment on a macroscopic length scale (scale bar is 5 μm; see also movie M9 in the Supporting Information). Trajectories of all tracked single molecules in (a) in the mesoporous silica structure (b). Scale bar is 5 μm.

position of the molecule was determined in each of the 1000 frames of the movie. In each frame, the position can be analyzed by simulating the point spread function of the fluorescent spot with a 2D Gaussian. The positioning accuracy depends on the signal-to-noise ratio and is typically in the range of 6−8 nm in our experiments (see also Figure 11b). The resulting trajectories are shown in Figure 10b for the corresponding pathways of the molecules in Figure 10a. These trajectories permit a detailed analysis of the movement of the molecules in the channels and give further information about the structure of these channels. As an example, we concentrated on the trajectory no. 1 in Figure 10. This trajectory is enlarged in Figure 11a and extends about 4 μm in the channel direction, which is chosen as the *x*-direction. In *y*-direction, however, it varies its width, being broad in the top region and thinning out toward the bottom region. This suggests that the molecule may not only travel up and down in a single channel but, in addition, may switch between neighboring channels through defects in the channel walls.

In order to analyze this in more detail, we determined the distribution of the positioning accuracy for this trajectory, which is depicted in Figure 11b. The histogram shows that the most likely positioning accuracy is 6−8 nm. This value is clearly smaller than the horizontal pore-to-pore distance (12−16 nm; see also Figure 9) and hence allows us to localize the dye molecule and distinguish its position from the position in a neighboring channel.

To analyze a possible switching of molecule no. 1 between adjacent channels, the *y*-axis was enlarged into the nanometer range while keeping the *x*-axis in the micrometer range. The plot of the trajectory in this axis system is shown in Figure 11c. It clearly indicates four different distinguishable regions in the *y* direction marked with four different colors. From this $x-y$ plot of the trajectory, the two separate graphs $x(t)$ and $y(t)$ can be obtained, shown in Figure 11d,e. They provide the movement of the molecule as a function of time separated in *x* and *y* direction.[13] From the graph $y(t)$ in Figure 11e, it is obvious that the molecule jumps in the *y* direction in four consecutive steps. These distributions can be fitted by four Gaussian curves with a maximum at 42.8 nm (black), 24.6 nm (red), 0.0 nm (blue), and 7.5 nm (green). The distances of these jumps can be correlated to jumps between adjacent channels. The corresponding channel structure in the $z-y$ plane is shown in Figure 11f. With this figure, the jumps of the molecule from region 1 (black) to region 4 (green) can be clearly interpreted as switches between adjacent channels. So the molecule starts in channel 1 and then jumps after 31.6 s through an adjacent channel to channel 2 where it then moves for further 93.9 s. Then it jumps again through an adjacent channel into channel 3 and stays there for an additional 39.2 s to finally jump into channel 4. For this pathway in *y* the jump widths correlate quite well with a horizontal mesochannel spacing of approximately 13 nm, which is in line with HR-SEM images shown in Figure 9. However, we cannot distinguish the ± direction of the jumps in *z*. Therefore, the jumps in the $-z$ direction could also occur in $+z$ or *vice versa*. From Figure 11f, it is obvious that the jumps from 1 to 2 and 2 to 3 have to occur in larger defects since they include at least two adjacent channels.

Additional information can be obtained from the graph $x(t)$ in Figure 11d. This plot shows that the molecule diffuses up and down within a range of approximately 1.5 μm in the first 165 s. The most striking pattern of this part of the trajectory is that the molecule frequently hits the same point at the upper and lower part in the *x* direction, indicating that there exist two blockades. Thus, the molecule is limited in its pathway along the channel direction by two dead ends. Interestingly, these dead ends seem to be nearly at the same position in *x* for the first two channels and may change somewhat for the third channel. When the molecule finally switches into channel 4 after 165 s, it finds a pathway that extends further in the *x* direction for more than 2.5 μm. So the molecule reaches the full extension of the trajectory in the *x* direction not in one channel but by switching into neighboring channels. A similar picture is obtained by the analysis of the other trajectories shown in Figure 10 (data not shown).

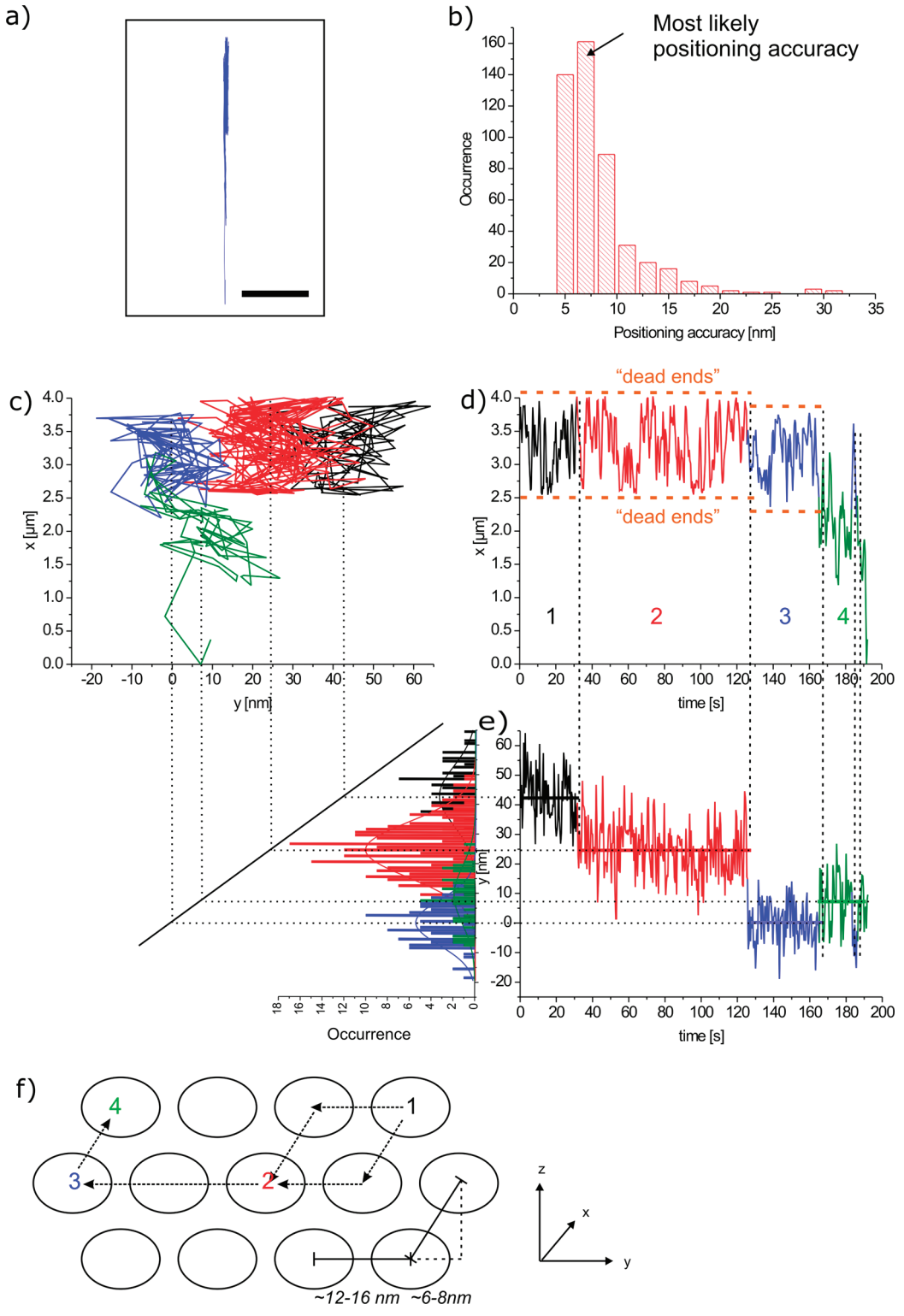

Figure 11. Detailed analysis of a trajectory in space and time. Trajectory of molecule no. 1 of the sample depicted in Figure 10 (sample 8) with its *x*-axis parallel to the pore direction, scale bar is 5 μm (a). Histogram of the positioning accuracy for this trajectory; the most likely positioning accuracy is 6−8 nm (b). Trajectory of molecule no. 1 with the *y*-axis in the nanometer range and the *x*-axis in the micrometer range for better clarity (c). Projection of *x* and *y* coordinates as a function of time for the single As-TDI molecule no. 1 shows diffusion of the molecule in at least four distinct neighboring pores (marked with black, red, blue, and green), while the molecule moves back and forth in each pore. Histograms of the *y* lateral coordinate (bottom left) for the four different time intervals with their Gaussian fits (black, 42.8 ± 1.0 nm; red, 24.6 ± 0.7 nm; blue, 0.0 ± 0.7 nm; green, 7.5 ± 0.2 nm) (d,e). A possible pathway of the single molecule, switching between neighboring channels (f).

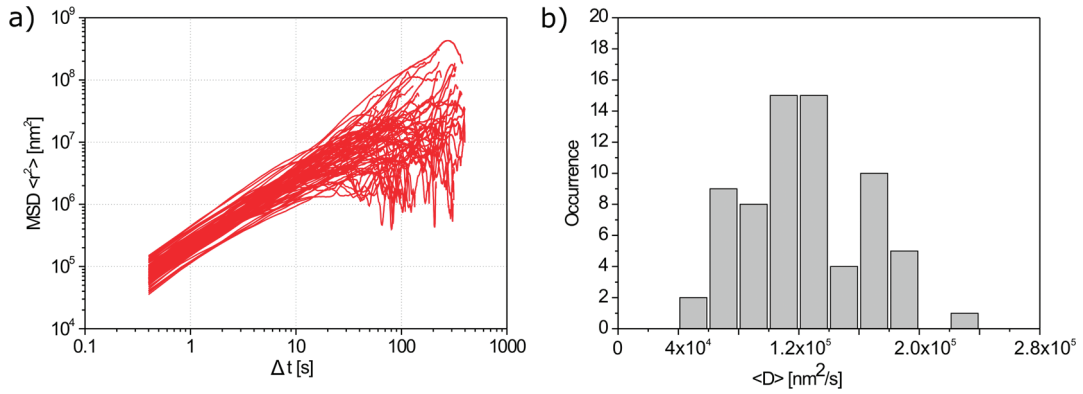

Figure 12. Statistical analysis of 70 molecular trajectories. Mean square displacements (MSD) *versus* time of 70 single-molecule trajectories (As-TDI) (a). Histogram of the mean diffusion coefficient $\langle D \rangle = 1.21 \times 10^5$ nm^2/s extracted from the linear part of the individual MSD plots for 70 As-TDI molecules (b).

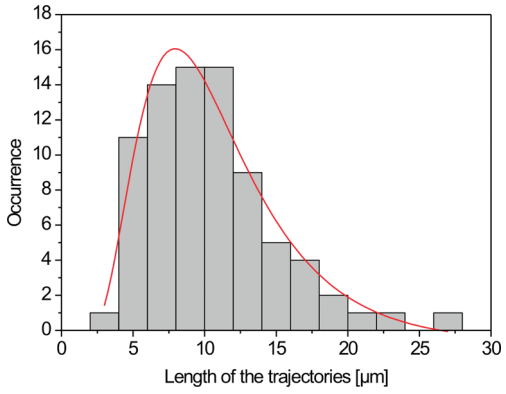

Figure 13. Histogram showing the length of the trajectories of 70 molecules within 400 s. The geometric mean and the multiplicative standard deviation of the fitted log-normal distribution (red line) are 9.0^x/1.6 μm.[22]

In summary, a molecule in such a mesoporous system mainly moves up and down along a single channel that may be blocked by imperfections. However, the molecule eventually finds a defect in the side wall which allows it to switch into a neighboring channel. There it can find its way further along the channel. The impact of imperfections that may block the pathway of molecules may be balanced by the defects in the side walls, allowing the molecule to circumvent dead ends. Thus, the molecule seems to move in a maze with channels oriented along one direction including some small openings to the side and blockades within the channels. This shows the *real structure* of the mesoporous system including its most relevant defects.

In addition to the structural details discussed above, our experiments reveal the dynamic properties of single molecules in such guest–host systems.[14] For this purpose, a statistical analysis based on the mean-square displacements (MSDs) as a function of time was performed for about 70 single-molecule trajectories for As-TDI. The resulting MSDs are plotted *versus* time Δt in Figure 12a.

The MSD graphs are approximately linear for at least the first 10 points (2 orders of magnitude in time) as expected for normal diffusion (Brownian motion). Therefore, it is possible to extract a diffusion coefficient using the relationship between MSD and time for a random walk in one dimension, as the molecules diffuse inside the highly oriented, parallel channels:

$$\text{MSD} = \langle r^2(t) \rangle = 2Dt$$

where D is the diffusion coefficient.

Most of the MSD plots are not perfectly linear for higher values of Δt but are slightly curved in the upper regime. This is a further indication of the presence of a confined diffusion, which is consistent with the presence of "dead ends" in the structure as discussed above.

The distribution of the diffusion coefficients for the 70 trajectories is shown in Figure 12b. It resembles a Gaussian curve with a mean diffusion coefficient of 1.21×10^5 nm^2/s, where the linear parts of the MSDs were fitted with a minor deviation of $\pm 2 \times 10^3$ nm^2/s. The diffusion coefficient of our samples is about 6 times higher for As-TDI than in other comparable known systems, such as Brij-56.[14] This can be mainly explained by the larger diameter of the pores used in this work (obtained with Pluronic F127 (Ø 6–8 nm) compared to Brij-56 (Ø 4–5 nm)). In addition, the different interactions between TDI/Brij-56 and TDI/F127 may influence the diffusion coefficient. Furthermore, the width of the distribution shows the heterogeneity of the mesoporous material; that is, it describes the large variation of the interactions between the molecules and their surroundings inside the channels.

The length of the accessible pores can be related to the resulting trajectories as discussed above.[11,12] Seventy molecules were observed, each for 1000 frames, which corresponds to an observation time of 400 s. In this time, the molecules can move up and down in the channels and switch between them. In order to characterize the possibility of a molecule to diffuse along

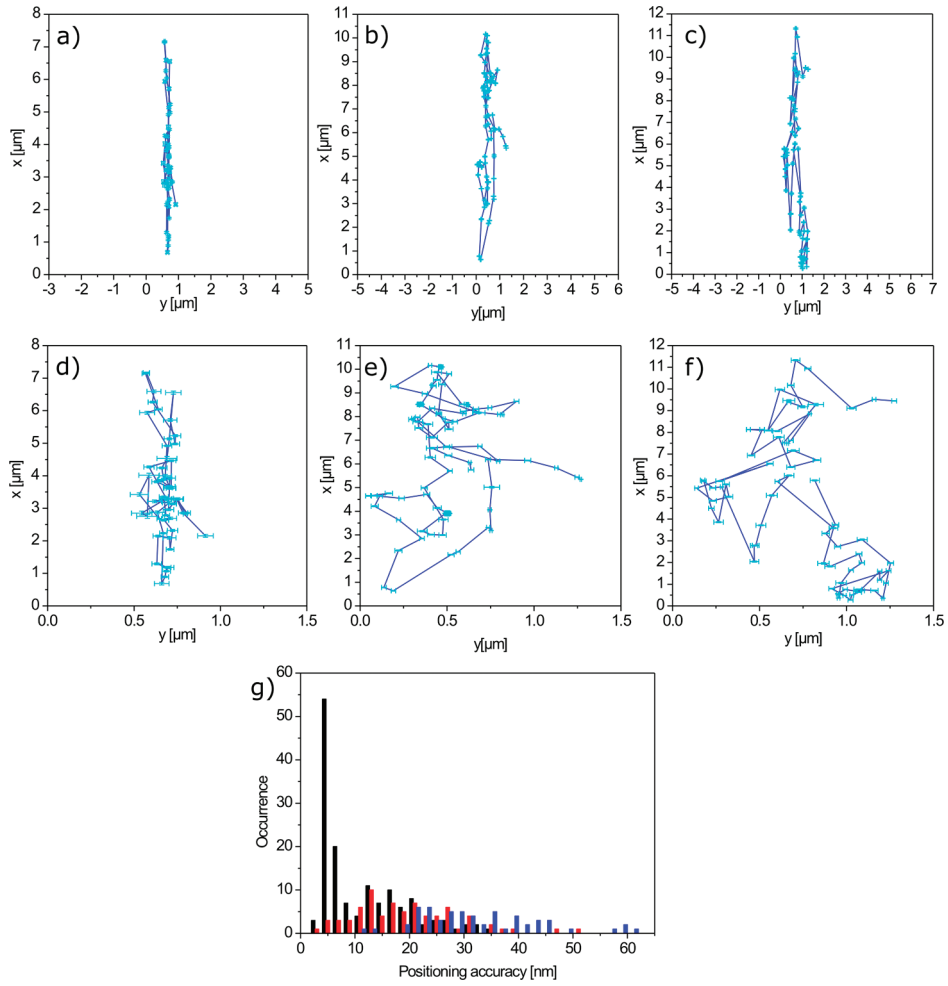

Figure 14. Trajectories of single fluorescent dye molecules reloaded into extracted mesoporous silica thin films and exposed to ethanol vapor. Trajectories in sample 9 (a,d) and sample 10 (b,c,e,f) are shown with an axis aspect ratio of 1 in (a−c) and a magnification of the *y*-axes for the same trajectories in (d−f). All axes are in micrometers. See also movie M10 (a,d) and M11 (b, c,e,f) in the Supporting Information. The positioning accuracy in these samples (blue (a,d), black (b,e), and red (c,f)) is plotted in the histogram below (g).

the channel direction in such a time, a statistical plot of the lengths of the trajectories is given in Figure 13. The broad distribution of the histogram in Figure 13 shows again the large heterogeneity of the system and was fitted with a log-normal function. The geometric mean and the multiplicative standard deviation of this log-normal distribution are $9.0^{x}/1.6\ \mu$m.[22]

The results discussed so far demonstrate how the quality of the mesoporous structure can be assessed directly from as-synthesized samples (*i.e.*, the dye molecules are diffusing inside the template-filled mesopores, and the PDMS stamp is not (necessarily) removed from the structures). For many applications, however, freely accessible mesopores that are not filled with a template are desired. The most common way to remove the template inside the pores is to calcine the material, typically at 400−500 °C. However, if the quality of the template-free structures is to be investigated by single-molecule fluorescence microscopy similar to the procedure shown above, calcination of the silica material is not an option since it usually results in a high background fluorescence that makes it impossible to identify single fluorophores. We found that this can be avoided by first extracting the template by refluxing in ethanol for 90 min before calcination. The resulting template-free mesoporous silica films can then again be loaded with various guest molecules. In order to examine the nature of the structure after this treatment, we loaded a fluorophore into the channels by submerging the films in an ethanolic solution of the dye at a concentration of approximately 10^{-10} to 10^{-11} M for a few hours under mild agitation, followed by rinsing in ethanol. During the incubation in the ethanolic dye solution, the fluorophores can enter the mesoporous network through open mesopores or defects in the structure. However, without a lubricant phase (like the template), the single dye molecules inside the mesoporous channels appear immobile because of strong interactions with active silanol groups at the walls of the channels (at least at the time scales we typically use for observation, *i.e.*, a

TABLE 1. Overview of the Samples Discussed in the Text[a]

sample code	microgroove height (μm)	surface properties of PDMS stamp	surface properties of glass substrate	microgroove filling method	aging conditions	post-treatment
1	2	hydrophilic	hydrophobic	capillary flow	48 h at rt and amb. hum.	none
2	2	hydrophilic	hydrophobic	capillary flow	48 h at rt and amb. hum.	none
3	2	hydrophobic	neutral (untreated)	stamping	48 h at rt and amb. hum.	none
4	2	hydrophilic	hydrophobic	capillary flow	48 h at rt and amb. hum.	none
5	2	hydrophilic	hydrophobic	capillary flow	48 h at rt and amb. hum.	removal of PDMS stamp
6	4–8	hydrophobic	hydrophilic	capillary flow	21 h at rt and sat. EtOH atm. and 24 h at rt and amb. hum.	none
7	4–8	hydrophobic	hydrophilic	capillary flow	21 h at rt and sat. EtOH atm. and 24 h at RT and amb. hum.	removal of PDMS stamp and standard SEM cross section preparation
8	4–8	hydrophobic	hydrophilic	capillary flow	21 h at rt and sat. EtOH atm. and 24 h at RT and amb. hum.	none
9	4–8	hydrophobic	hydrophilic	capillary flow	21 h at rt and sat. EtOH atm. and 24 h at rt and amb. hum.	removal of PDMS stamp, incubation in NH_3-atm., extraction in EtOH (reflux), calcination in air
10	4–8	hydrophobic	hydrophilic	capillary flow	21 h at rt and sat. EtOH atm. and 24 h at rt and amb. hum.	removal of PDMS stamp, incubation in NH_3-atm., extraction in EtOH (reflux), calcination in air

[a] See the Materials and Methods part for further details on the entries of the table; rt = room temperature (typically 22–25°C); amb. hum. = ambient humidity (typically 30–60%); atm. = atmosphere.

few minutes). In order to enable dye movement inside the pores, an atmosphere of an organic solvent such as ethanol or chloroform (good solvents for As-TDI) is required, which results in the formation of a lubricant-like phase inside the pores. In the presence of such a solvent atmosphere, dye molecules inside the pores usually move much faster and also tend to photobleach more rapidly than in unextracted samples. However, it is still possible to follow the movement of single dye molecules and thus obtain the corresponding trajectories indicating the pathways in the mesoporous silica network, as explained above (Figure 14). These trajectories indicate that there still is a preferential direction of diffusion; however, by comparing the trajectories to those shown in Figure 10, it is obvious that there are more defects in the silica network after this treatment.

CONCLUSIONS

In this study, we have demonstrated that well-defined macroscopic alignment of Pluronic F127-templated, large-pore mesochannels in mesoporous silica can be achieved by confinement in PDMS microgrooves. The influence of various experimental conditions including the way the channels are filled, the surface modification at the solid/liquid interfaces, and the aspect ratio of the microgrooves were investigated. Furthermore, we found that the alignment of the mesochannels can change abruptly from parallel to perpendicular depending on the height within the microgrooves.

We also show how single-molecule fluorescence microscopy can be used to directly assess the mesopore structure of the as-synthesized silica thin films, how a maximum projection can give a global overview on the pore structure, how it can give deeper insights into the real microscopic structure of the mesoporous silica framework, and how it can help us to gain dynamic information about the diffusion of guest molecules inside these compounds. The spatial accuracy in these experiments is high enough to observe movements of the dye molecules between individual channels in the mesoporous silica. This high resolution allows us to observe details of long-distance movement of the molecules: in order to travel the very large distances in these highly ordered structures, the molecules circumvent

defects by moving to neighboring channels. Finally, we illustrate how solvent-extracted samples can be investigated by this technique and how the defect concentration increases as a result of template removal.

MATERIALS AND METHODS

If not stated otherwise, all chemicals were used as received. Absolute ethanol, tetraethylorthosilicate (TEOS), and Pluronic F127 were purchased from Sigma-Aldrich Co. HCl (1 M) was purchased from AppliChem GmbH. Standard glass coverslips (#1, 22 × 22 mm^2) were purchased from Gerhard Menzel, Glasbearbeitungswerk GmbH & Co. KG. Hellmanex cleaning solution was purchased from Hellma GmbH & Co. KG. PDMS and PDMS curing agent were purchased from Dow Corning Co. 1*H*,1*H*,2*H*,2*H*-Perfluorooctyltriethoxysilane (PFOTS) was purchased from abcr GmbH & Co. KG. Aqueous ammonium hydroxide solution (25%) was purchased from VWR International GmbH.

Exposure to oxygen plasma was carried out with a Femto Plasma System from Diener Electronic typically operated at a power of 50 W and an oxygen flow of 4−5 sccm. Atomic force microscopy (AFM) images were recorded with a Nanoink NScriptor DPN System in close contact mode. One-dimensional X-ray diffraction (XRD) patterns were obtained with a Bruker D8 Discover X-ray diffractometer using Cu Kα radiation. Scanning electron microscopy (SEM) and high-resolution scanning electron microscopy (HR-SEM) images were obtained with a JEOL JSM6500F scanning electron microscope equipped with a field-emission gun, typically operated at an acceleration voltage of 4 and 10 kV and a working distance of 10 and 7 mm for SEM and HR-SEM, respectively. Single-molecule fluorescence images of the as-synthesized samples with the PDMS stamp still in place were recorded with a wide-field setup, using an Eclipse TE200 (Nikon) epi-fluorescence microscope with a high numerical aperture (NA) oil-immersion objective (Nikon Plan Apo, 100×, NA = 1.40). The fluorescent dye *N*-(2,6-diisopropylphenyl)-*N*′-octylterrylene-3,4,11,12-tetracarboxdiimide (called As-TDI in this work; for the chemical structure, see Figure 1 and ref 16) with a high photostability and excellent quantum yield were incorporated into the material in single-molecule concentrations (10^{-10} to 10^{-11} mol/L). The dye was kindly provided by the research group of Prof. Klaus Müllen (Max-Planck-Institute for Polymer Research, Mainz, Germany).

The molecules were excited at 633 nm with a He−Ne gas laser (Coherent, 75 mW maximum at 632.8 nm) with an intensity of 0.3 kW cm^{-2}. Their fluorescence was detected with a back-illuminated electron multiplying charge-coupled device (EM-CCD) camera in frame transfer mode (Andor iXon DV897). Incident laser light was blocked by a dichroic mirror (640 nm cutoff, AHF) and a band-pass filter (730/140 AHF). One pixel on the camera chip corresponds to 154 nm on the sample. The individual molecule patterns were fitted by a Gaussian function

$$f_1(x, y, A, w) = A \times e^{-\left(\frac{x - x_0}{w}\right)^2} \times e^{-\left(\frac{y - y_0}{w}\right)^2}$$

where *A* and *w* are the amplitude and the width of the Gaussian curve, respectively. The method was described in detail in previous studies.[11,17,18] The resulting positions can be combined frame by frame to form molecular trajectories as described in the text.

The EISA precursor solution was prepared following a procedure from Okubo *et al.*[15] with slight modifications. First, 700 μL of Millipore water and 100 μL of HCl (1 M) were mixed with 4.4 g of ethanol (abs.) and 1.0 g of tetraethylorthosilicate (TEOS) and stirred at 65 °C for 1 h in a sealed polypropylene beaker. At the same time, 475 mg of Pluronic F127 was mixed with 4.4 g of ethanol and stirred at room temperature for 1 h. Then, the surfactant solution was added to the silica solution, and the resulting clear liquid of molar composition 1.00:7.37 × 10^{-3}:39.8:2.19 × 10^{-2}:9.27 (TEOS/F127/ethanol/HCl/water) was stirred for another 2−4 h at room temperature. PDMS stamps were fabricated by replica molding from photolithographically patterned masters using standard techniques. The final thickness of the stamps was typically about 1.0−1.5 mm. The substrates were cleaned by submerging them in a water/Hellmanex solution at 60 °C for 1 h, followed by ultrasonic agitation for 3 min and rinsing with DI water. For further surface modification, the cleaned substrates were treated by submersion in piranha solution for 1 h or by exposing them to oxygen plasma for 15 min. When hydrophilic substrates were desired, the substrates were directly used after this treatment. For hydrophobic substrates, the activated glass coverslips were placed in a desiccator alongside a Petri dish with 1*H*,1*H*,2*H*,2*H*-perfluorooctyltriethoxysilane (PFOTS), the pressure was reduced until the boiling pressure of the silane was reached at ambient temperature (approximately 7 × 10^{-2} mbar), and the substrates were incubated in the resulting silane atmosphere for 3−4 h. When hydrophobic stamps were desired, the PDMS replica molds were used without further modifications because PDMS is intrinsically hydrophobic. To render the PDMS hydrophilic, it was exposed to oxygen plasma for 90 s and then submerged in an aqueous solution of TEOS (3 mM) and HCl (96 mM) for 2 h. It is well-known that functionalized trialkoxy- and trichlorosilanes can be grafted to reactive surface hydroxyl groups from the liquid or the gas phase.[19,20]

In some cases, extraction of the template was achieved by refluxing the samples in ethanol (abs.) for 90 min after they had been subjected to an NH_3 atmosphere obtained by incubating the samples in a closed container next to a Petri dish containing an ammonium hydroxide solution (25% in water) at room temperature for 10−15 min (to promote silica condensation). Subsequently, the samples were calcined in air by first heating at 60 °C for 90 min (ramp: 1 °C/min), then at 160 °C for 90 min (ramp: 1 °C/min), and finally at 400 °C for 4 h (ramp: 1 °C/min).

An overview of the different samples discussed in this work including precise treatment and synthesis conditions can be found in Table 1.

Conflict of Interest: The authors declare no competing financial interest.

Acknowledgment. We thank K. Müllen for providing the TDI dye molecule. Moreover, we thank Y. Xiang, G. Abstreiter, M. Firnkes, and U. Rant from the Technische Universität München for their help with creating the masters for the PDMS stamps. Fruitful discussions with J. Michaelis (University of Ulm) are much appreciated. Financial support from SFB 749 and the cluster of excellence Nanosystems Initiative Munich (NIM) is gratefully acknowledged.

Supporting Information Available: M1: Movie recorded with a fluorescence microscope at a frame rate of 2.5 fps taken from sample **1** (false-colored in blue; scale bars are 5 μm; see also Figure 1). M2: Movie recorded with a fluorescence microscope at a frame rate of 2.5 fps taken from sample **1** (false-colored in blue; scale bars are 5 μm; see also Figure 1). M3: Movie recorded with a fluorescence microscope at a frame rate of 2.5 fps taken from sample **2** (false-colored in blue; scale bars are 5 μm; see also Figure 2 and Figure 5). M4: Movie recorded with a fluorescence microscope at a frame rate of 2.5 fps taken from sample **3** (false-colored in blue; scale bars are 5 μm; see also Figure 4). M5: Movie recorded with a fluorescence microscope at a frame rate of 2.5 fps taken from sample **4** (false-colored in blue; scale bars are 5 μm; see also Figure 5). M6: Movie recorded with a fluorescence microscope at a frame rate of 2.5 fps taken from sample **2** (false-colored in blue; scale bars are 5 μm; see also Figure 6). M7: Movie recorded with a fluorescence microscope at a frame rate of 2.5 fps taken from sample **6** (false-colored in blue; scale bars are 5 μm; see also Figure 8). M8: Movie recorded with a fluorescence microscope at a frame rate of 2.5 fps taken

from sample **6** (false-colored in blue; scale bars are 5 μm; see also Figure 8). M9: Movie recorded with a fluorescence microscope at a frame rate of 2.5 fps taken from sample **8** (false-colored in blue; scale bars are 5 μm; see also Figure 10). M10: Movie recorded with a fluorescence microscope at a frame rate of 2.5 fps taken from sample **9** (false-colored in blue; scale bars are 5 μm; see also Figure 14). M11: Movie recorded with a fluorescence microscope at a frame rate of 2.5 fps taken from sample **10** (false-colored in blue; scale bars are 5 μm; see also Figure 14). This material is available free of charge *via* the Internet at http://pubs.acs.org.

REFERENCES AND NOTES

1. Fan, R.; Huh, S.; Yan, R.; Arnold, J.; Yang, P. Gated Proton Transport in Aligned Mesoporous Silica Films. *Nat. Mater.* **2008**, *7*, 303–307.
2. Luo, H.; Wang, D.; He, J.; Lu, Y. Magnetic Cobalt Nanowire Thin Films. *J. Phys. Chem. B* **2005**, *109*, 1919–1922.
3. Yang, P.; Wirnsberger, G.; Huang, H. C.; Cordero, S. R.; McGehee, M. D.; Scott, B.; Deng, T.; Whitesides, G. M.; Chmelka, B. F.; Buratto, S. K.; *et al.* Mirrorless Lasing from Mesostructured Waveguides Patterned by Soft Lithography. *Science* **2000**, *287*, 465–467.
4. Kresge, C. T.; Leonowicz, M. E.; Roth, W. J.; Vartuli, J. C.; Beck, J. S. Ordered Mesoporous Molecular Sieves Synthesized by a Liquid-Crystal Template Mechanism. *Nature* **1992**, *359*, 710–712.
5. Wu, C.-W.; Ohsuna, T.; Edura, T.; Kuroda, K. Orientational Control of Hexagonally Packed Silica Mesochannels in Lithographically Designed Confined Nanospaces. *Angew. Chem., Int. Ed.* **2007**, *46*, 5364–5368.
6. Kim, E.; Xia, Y.; Whitesides, G. M. Polymer Microstructures Formed by Moulding in Capillaries. *Nature* **1995**, *376*, 581–584.
7. Trau, M.; Yao, N.; Kim, E.; Xia, Y.; Whitesides, G. M.; Aksay, I. A. Microscopic Patterning of Orientated Mesoscopic Silica through Guided Growth. *Nature* **1997**, *390*, 674–676.
8. Tolbert, S. H.; Firouzi, A.; Stucky, G. D.; Chmelka, B. F. Magnetic Field Alignment of Ordered Silicate-Surfactant Composites and Mesoporous Silica. *Science* **1997**, *278*, 264–268.
9. Miyata, H.; Kuroda, K. Preferred Alignment of Mesochannels in a Mesoporous Silica Film Grown on a Silicon (110) Surface. *J. Am. Chem. Soc.* **1999**, *121*, 7618–7624.
10. Zhao, D.; Yang, P.; Melosh, N.; Feng, J.; Chmelka, B. F.; Stucky, G. D. Continuous Mesoporous Silica Films with Highly Ordered Large Pore Structures. *Adv. Mater.* **1998**, *10*, 1380–1385.
11. Kirstein, J.; Platschek, B.; Jung, C.; Brown, R.; Bein, T.; Bräuchle, C. Exploration of Nanostructured Channel Systems with Single-Molecule Probes. *Nat. Mater.* **2007**, *6*, 303–310.
12. Zürner, A.; Kirstein, J.; Döblinger, M.; Bräuchle, C.; Bein, T. Visualizing Single-Molecule Diffusion in Mesoporous Materials. *Nature* **2007**, *450*, 705–708.
13. Jung, C.; Kirstein, J.; Platschek, B.; Bein, T.; Budde, M.; Frank, I.; Müllen, K.; Michaelis, J.; Bräuchle, C. Diffusion of Oriented Single Molecules with Switchable Mobility in Networks of Long Unidimensional Nanochannels. *J. Am. Chem. Soc.* **2008**, *130*, 1638–1648.
14. Feil, F.; Jung, C.; Kirstein, J.; Michaelis, J.; Li, C.; Nolde, F.; Müllen, K.; Bräuchle, C. Diffusional and Orientational Dynamics of Various Single Terylene Diimide Conjugates in Mesoporous Materials. *Microporous Mesoporous Mater.* **2009**, *125*, 70–78.
15. Naik, S. P.; Yamakita, S.; Ogura, M.; Okubo, T. Studies on Mesoporous Silica Films Synthesized Using F127, a Triblock Co-polymer. *Microporous Mesoporous Mater.* **2004**, *75*, 51–59.
16. Holtrup, F. O.; J., G. R.; Quante, H.; Feyter, S. D.; De, F. C.; Müllen, K. Terrylenimides: New NIR Fluorescent Dyes. *Chem.—Eur. J.* **1997**, *3*, 219–225.
17. Hellriegel, C.; Kirstein, J.; Bräuchle, C. Tracking of Single Molecules as a Powerful Method To Characterize Diffusivity of Organic Species in Mesoporous Materials. *New J. Phys.* **2005**, *7*, 1–14.
18. Hellriegel, C.; Kirstein, J.; Bräuchle, C.; Latour, V.; Pigot, T.; Olivier, R.; Lacombe, S.; Brown, R.; Guieu, V.; Payrastre, C.; *et al.* Diffusion of Single Streptocyanine Molecules in the Nanoporous Network of Sol−Gel Glasses. *J. Phys. Chem. B* **2004**, *108*, 14699–14709.
19. Sharma, V.; Dhayal, M.; Govind; Shivaprasad, S.; Jain, S. Surface Characterization of Plasma-Treated and PEG-Grafted PDMS for Micro Fluidic Applications. *Vacuum* **2007**, *81*, 1094–1100.
20. Duez, C.; Ybert, C.; Clanet, C.; Bocquet, L. Making a Splash with Water Repellency. *Nat. Phys.* **2007**, *3*, 180–183.
21. Daiguji, H.; Tatsumi, N.; Kataoka, S.; Endo, A. One-Dimensional Alignment of SBA-15 Films in Microtrenches. *Langmuir* **2009**, *25*, 11221–11224.
22. Limpert, E.; Stahel, W. A.; Abbt, M. Log-Normal Distributions across the Sciences: Keys and Clues. *BioScience* **2001**, *51*, 341–352.